frontiers | Frontiers in Earth Science

TYPE Original Research
PUBLISHED 26 January 2023
DOI 10.3389/feart.2023.1120618

OPEN ACCESS

EDITED BY
Chengyi Pu,
Central University of Finance and Economics, China

REVIEWED BY
Yang Xian,
China University of Geosciences Wuhan, China
Yunfeng Dai,
Nanjing Hydraulic Research Institute, China
Chenxi Wang,
University of Waterloo, Canada

*CORRESPONDENCE
Qiang Zhang,
zhangq@cdut.edu.cn

SPECIALTY SECTION
This article was submitted to Environmental Informatics and Remote Sensing, a section of the journal Frontiers in Earth Science

RECEIVED 10 December 2022
ACCEPTED 16 January 2023
PUBLISHED 26 January 2023

CITATION
Qin Z, Zhang Q, Yu S, Yang Y, Zhang J, Xu M, Liu Y, Liu M and Nie M (2023), Revealing karst water circulation based on the GIS and environmental isotopes methods—A case study in eastern Sichuan, southwestern China.
Front. Earth Sci. 11:1120618.
doi: 10.3389/feart.2023.1120618

Revealing karst water circulation based on the GIS and environmental isotopes methods—A case study in eastern Sichuan, southwestern China

Zixuan Qin[1], Qiang Zhang[1]*, Siyao Yu[1], Yanna Yang[1], Jiasen Zhang[1], Mo Xu[1], Yang Liu[2], Maoyi Liu[3] and Mi Nie[3]

[1]State Key Laboratory of Geohazard Prevention and Geoenvironment Protection, College of Environment and Civil Engineering, Chengdu University of Technology, Chengdu, China, [2]Chongqing Survey Institute, Chongqing, China, [3]Chongqing Urban Infrastructure Construction Co., Ltd., Chongqing, China

Jura-type folds in eastern Sichuan Basin have created unique multi-type karst water circulation patterns. Understanding the karst water circulation features is helpful to the protection and management of water resources in this area. In this study, a typical Jura-type fold Mingyueshan in eastern Sichuan, Southwestern China is taken as an example. The geological conditions, natural geographical factors, and environmental isotopes data (δ^2H, δ^{18}O, δ^3H) are analyzed, the GIS method was used to construct the groundwater flow system. The results reveal the karst water circulation patterns under the control of multiple drainage base levels. Finally, it comes to the conclusion that the north, middle and south sections of Mingyueshan present three water circulation patterns: unidirectional shallow circulation system, bidirectional shallow circulation system and unidirectional shallow-deep nested circulation system, respectively. These results are essentially qualitative, some numerical simulations of groundwater flow can be considered in future work, which will help to determine the groundwater flow system quantitatively. The research results can provide reference for the studies of karst aquifers in eastern Sichuan Jura-type folds area and other areas with similar characteristics.

KEYWORDS

Jura-type fold Mingyueshan, karst water circulation patterns, GIS, drainage base level, environmental isotopes

1 Introduction

Karst is widely distributed all over the world, which cover 7%–12% of the Earth's land surface, meanwhile, karst aquifers contain rich fresh water resources (Ford and Williams, 2007; Lorette et al., 2018; Liu et al., 2021). Therefore, it is essential to accurately grasp the groundwater circulation characteristics in karst area. The groundwater flow theory creatively proposed by Tóth (1962) and Tóth (1963) gives better description of the law of regional groundwater circulation, which does not completely depend on the geological factors, and it is also controlled by the natural geographical factors (Tóth, 2009; Liang et al., 2012; Liang et al., 2022). Different groundwater flow systems have different flow mechanics characteristics, there are great differences in water chemistry and isotopes. Although the strong spatial heterogeneity of karst aquifers causes challenges for research, existing studies have shown that hydrogen and oxygen isotopes can perform well in complex karst water systems (Kattan, 1997; Vasic et al., 2019; Gil-Marquez et al., 2019; Torresan et al., 2020; Deng et al., 2022; Ma et al., 2022), which

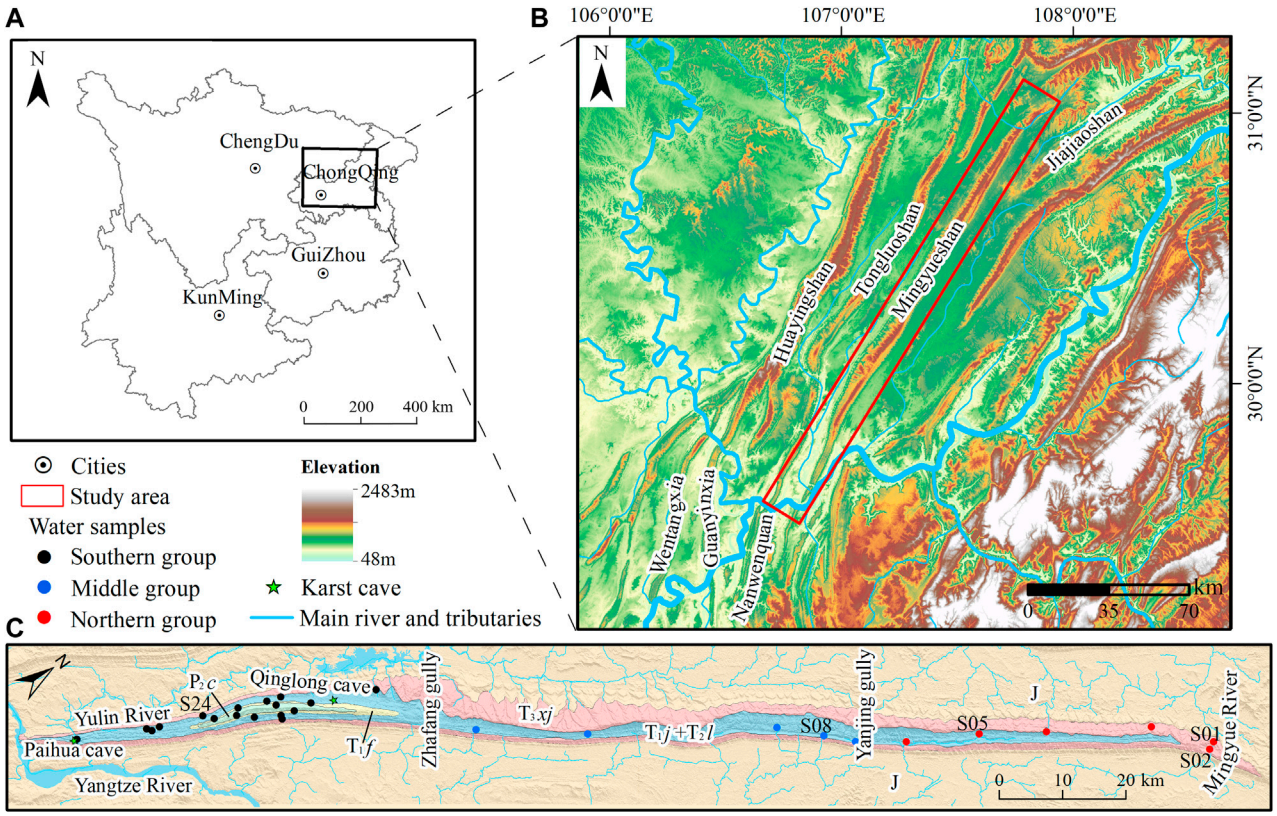

FIGURE 1
(A) Map of study area. **(B)** Altitude DEM rendering map of study area. **(C)** Overview map of the study area indicating water samples.

provides a theoretical basis for application of hydrogen and oxygen environmental isotopes to reveal karst water flow systems.

The Jura-type folds, also known as the detachment folds, which evaporates incompetent Triassic and develops a serial of parallel "comb-like and trough-like" folds (Laubscher, 1977; Wang et al., 2012). Typical examples are the Jura Mountains of the Swiss, the foreland region of the Appalachian Orogenic Belt, the foreland region of the Cordillera Orogenic Belt (Rich, 1934; Davis, 1980; Suppe, 1983). A serial of NNE–SSW trending "comb-like and trough-like" fold belts in eastern Sichuan Basin are caused by multi-layer detachment, belonging to typical Jura-type folds (Wang et al., 2010; Wang et al., 2022). The concrete manifestation is that the soluble rock is exposed in the core of the high-steep anticline and the east and west limbs are clamped by the relative water-isolated sandstone and mudstone. Under this special tectonic condition, the near east-west (EW) direction gullies, or transverse gullies briefly, largely control the groundwater discharge and circulation in karst mountainous areas. Neotectonic movement caused regional crustal uplift, resulting in continuous downward cutting of the hydrological network and the development of transverse rivers with different cutting depths and lengths. According to the degree of transverse gullies cutting through the soluble rock strata, they can be divided into three types: fully-cut, partly-cut, and uncut gully. Typical Jura-type folds in eastern Sichuan Basin such as Wentangxia, Huayinshan, Tongluoshan, Mingyueshan, and Jiajiaoshan show a variety of gully cutting and groundwater drainage types. Up till to now, there are many studies on karst aquifers in the Jura-type folds area of the eastern Sichuan Basin. However, existing studies mainly focus on the physicochemical properties, occurrence condition or quality evaluation of karst water (Pu et al., 2014; Xiao et al., 2018; Chen et al., 2020; Zhang et al., 2022), few researches pay attention to karst water cycle pattern in this area. To be more specific, how multiple drainage base levels and their combinations affect and control the karst water circulation in this area remains a question worth exploring.

In this study, theoretical controlling factors of karst water flow, the GIS method and environmental isotopes data were analyzed to reveal the karst water circulation patterns under the control of different drainage base levels in Mingyueshan. Finally, the different karst water circulation patterns in the north, middle and south sections of the Mingyueshan was summarized. This work is beneficial to the management of water resources and the safety of underground engineering in the study area, provides reference for the study of karst aquifers with similar characteristics in eastern Sichuan Jura-type folds area and other area.

2 Study area

2.1 Physical geography conditions

The Mingyueshan, located on the Chongqing Municipality, lies between latitudes 29°28′–31°01′ N and longitudes 106°45′–107°56′ E.

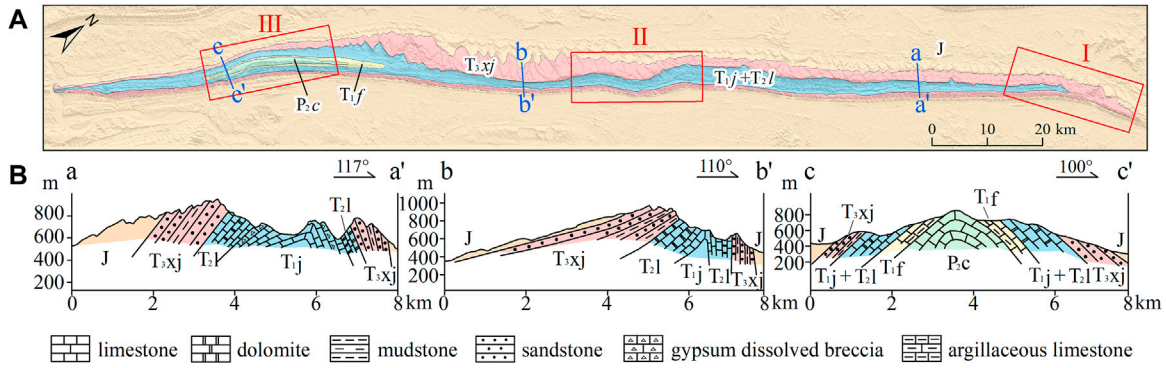

FIGURE 2
(A) Structural trace of Mingyueshan anticline. **(B)** Two limbs morphology shown in sections a–a′, b–b′, and c–c′.

It is a 210-km typical eastern Sichuan Jura-type fold with narrow axis and asymmetrical limbs. The Yulin river and the Mingyue river pass through the south and north of the long anticline, respectively (Figure 1).

The study area is controlled by the semitropical climate, with distinct seasons. The average temperature is 16°C–18°C throughout the year. The rainfall is abundant and there is an obvious vertical zonation of rainfall, in which the average annual rainfall in the basin and river valley is about 998 mm, while the rainfall in the mountain area exceeds 1,100 mm (Yang et al., 2019). The river systems in the study area are well developed with a dendritic distribution.

2.2 Geological conditions

The Eastern Sichuan fold-thrust belt (ESFTB) is situated in the eastern margin of the middle and upper Yangtze blocks in the South China Craton (Charvet, 2013; Lu et al., 2014). It had experienced Yanshan and Himalayas movement, then developed a serial of NNE–SSW trending asymmetric high-steep folds, one of which is Mingyueshan anticline. The Mingyueshan anticline is located in the southwest area of ESFTB, which is a narrow and long structural belt and subjected to the combined action of west-east compression and bottom-up uplift during the tectonic deformation. Therefore, the structural features and two limbs of the north, middle and south parts are presented differently (Figure 2).

The northern part of Mingyueshan was affected by the southward thrust and nappe of the South Dabashan mountains tectonic belt in the north of Mingyueshan, leading to the south-east bending of Mingyueshan fold belt and its continued northward expansion. The influence of the southward thrust and nappe of the South Dabashan mountains was getting more intense (Wen and Li, 2020). As a result, the limbs of the northern anticline are roughly symmetrical (Figure 2A and section a–a′). In the middle part, the lithology phase transition occurred in part of the area, the difference of lithology led to the concentration of stress and displacement, appearance of multiple rotation axis segments. The rock strata in the west limb of the middle part were inclined gently, while the rock strata in the east limb were steep (Figure 2B and section b–b′). In the southern part, affected by the thickness of the weak layer (detachment layer), the tectonic stress and displacement were more likely to transfer to the west along the detachment layer, resulting in the uplift of the anticlinal core. The difference in detachment layer thickness led to a significant difference in the transfer of tectonic deformation from east to west in the study area. The two limbs of the south part were roughly symmetrical (Figure 2C and section c–c′).

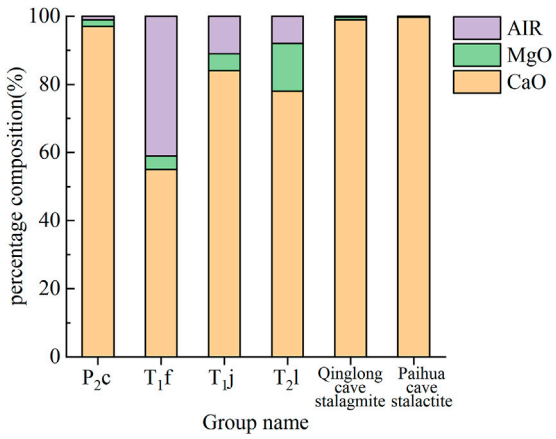

FIGURE 3
Carbonated rocks composition of water-bearing formation and two karst caves.

The soluble rocks in the anticline are only exposed in the core area, while the east and west limbs are clamped by the water-isolated sandstone and mudstone of the Upper Triassic Xujiahe Formation (T_3xj) (Chen et al., 2016; Szczygieł et al., 2018). The soluble rocks in the northern part are mainly limestone and dolomite in the Middle Triassic Leikoupo (T_2l) and the Lower Triassic Jialingjiang Formations (T_1j), with a small amount of gypsum dissolved breccia. The middle part has the same soluble rock lithology as the north part, which consists of limestone and dolomite. In addition to Leikoupo and Jialingjiang Formation, there are argillaceous limestone of the Upper Permian Changxing Formation (P_2c) and the Lower Triassic Feixianguan Formation (T_1f) in the anticline core of the southern soluble rocks (Figure 2). The carbonated rocks composition such as CaO, MgO and AIR (acid-insoluble residue) of water-bearing formation and two caves in the Mingyueshan area is shown in Figure 3.

3 Methods

3.1 Tóth's groundwater flow system built by the GIS

Tóth (1962) and Tóth (1963) obtained the groundwater flow system in a basin of undulating topographic surface by analytical solution. Tóth's study showed the nested groundwater systems of local, intermediate, and regional flow systems, discussed the geological force of groundwater flow (Tóth, 1999). In general, groundwater circulation is not entirely dependent on geological factors, but also controlled by natural geographical factors such as topographic potential energy and drainage system (Tóth, 2009; Liang et al., 2012; Liang et al., 2022). The difference of topographic potential energy is the main driving force of groundwater movement. Recharge areas with high terrain accumulate potential energy with recharge, while discharge area with low-lying terrain is difficult to accumulate potential energy. Therefore, topography usually controls the spatial distribution of topographic potential energy.

During the intermittent uplift of crust, the karst water circulation is closely related to the evolution of karst topography (Hill and Polyak, 2010). On the one hand, the evolution of karst topography is a process that changes with time, the alternate water cycle conditions control the evolution of karst topography. On the other hand, topographical control over hydrology can be manifested in a short period of time. The diversity and difference of karst landforms lead to different hydrological functions of karst systems, groundwater shows regional and local drainage characteristics. In order to obtain the relationship between karst topography and hydrological system clearly in the study area, transverse gully cut points and karst depressions were extracted automatically using digital elevation model (DEM) and geographic information system (GIS) data (Pavel et al., 2016; Wu et al., 2016; Meng et al., 2018).

3.2 Environmental isotopes

3.2.1 Water sampling

Water sampling campaigns were conducted in the study area during the period of 27th August to 2nd September 2018 (sampling sites are shown in Figure 1). A total of 33 groups of samples were collected from the north, middle and south parts of Mingyueshan for environmental isotope testing, among which 28 groups from all sampling sites were tested for δ^2H and $\delta^{18}O$ isotope, and the rest, five groups were tested for δ^3H isotope, marked as from S01, S02, S05, S08 and S24 sites. Sampling bottles were rinsed with sample water at least five times before collection. The water samples collected in the field being sealed in 500 mL polyethylene bottles and stored in a low-temperature environment above zero. The samples were sent to the Institute of Karst Geology, Chinese Academy of Geological Sciences for isotope testing within 7 days after collection. δ^2H and $\delta^{18}O$ were tested by MAT253 stable isotope mass spectrometer, tritium was tested by Qnantulus1220 ultra-low local liquid scintillation spectrometer.

3.2.2 δ^3H dating

Environmental isotope tritium is a radioactive isotope of hydrogen with a half-life of 12.43a (Lucas and Unterweger 2000). Generally, the tritium content in groundwater is only affected by the decay rule, does not exchange with rock medium. Therefore, it is often used as the tracer signal of precipitation input to study the dating of groundwater (Solomon and Sudicky 1991; Kaufman et al., 2003; Gleeson et al., 2016; Cauquoin et al., 2017). Relevant studies show that the annual variation curve of tritium concentration in global atmospheric precipitation has similar morphological characteristics, there is correlation between the data (Taylor 1966; Koster et al., 1989; Michel 1989). Therefore, the application of factor analysis method to the analysis of the average annual tritium concentration in atmospheric precipitation has a longer time and larger space applicability (Doney et al., 1992; Zhang et al., 2011). The MGMTP (Yang and Ye 2018) model of factor analysis was used to recover the annual average tritium concentration of atmospheric precipitation in the study area from 1953 to 2018.

Groundwater in Chongqing area is mainly replenished by atmospheric rainfall. The tritium values of atmospheric precipitation in the study area from 1953 to 2017 are taken as the input function, the piston flow model (PFM) of a single input-output system is calculated and selected to establish the relationship between the groundwater output age and the tritium output concentration. The PFM assumes that groundwater flow in an ideal aquifer is similar to piston motion, i.e. equal-scale mixing model, which means that the recharge is punctual and all tracer concentrations arrive as a unique peak without mixing between flow lines (Nir, 1964; Silva and Cota, 2021). Therefore, the retention age of groundwater can be deduced by measuring the tritium value of the samples.

$$C_{out}(t) = C_{in}(t-\tau)e^{-\lambda\tau}$$

where, t is the time series of isotope output; τ is the transmission time of isotope, i.e., the age. $t-\tau$ is isotope input time series. $C_{out}(t)$ is the tritium output function of groundwater system. $C_{in}(t-\tau)$ is the tritium input function of groundwater system. λ is the tritium decay constant, equals to 0.055764.

4 Results and discussions

4.1 Karst hydro-geomorphology

Transverse gully cut points and karst depressions were extracted (Figure 4) and the elevation and development density of transverse gullies were calculated (Table 1) in each part of Mingyueshan. From north to south, the number of transverse gullies cut points increase, the depth of karst depression changes from shallow to deep, the development density and range of karst depressions also increase. In the area close to the fully-cut gully, groundwater circulation gradually adapts to the downward cutting of the fully-cut gully, the surface basically has no gully development, then the partly-cut gully loses the drainage ability. The terrain landform of the study area is obviously controlled by the geological structure and lithologic characteristic, the groundwater migrates mainly along the tectonic line from north to south to the Yulin river (the primary tributary of the Yangtze river), the lowest drainage base level. The dynamic conditions of groundwater are mainly controlled by the Yulin river which fully cuts through the anticline karst formation, the gullies, which partly cut into the anticline karst rock.

The depth of groundwater circulation is largely determined by the relative height of recharge and discharge zones (Stringfield et al., 1979). Under the unique background of the Jura-type folds in eastern

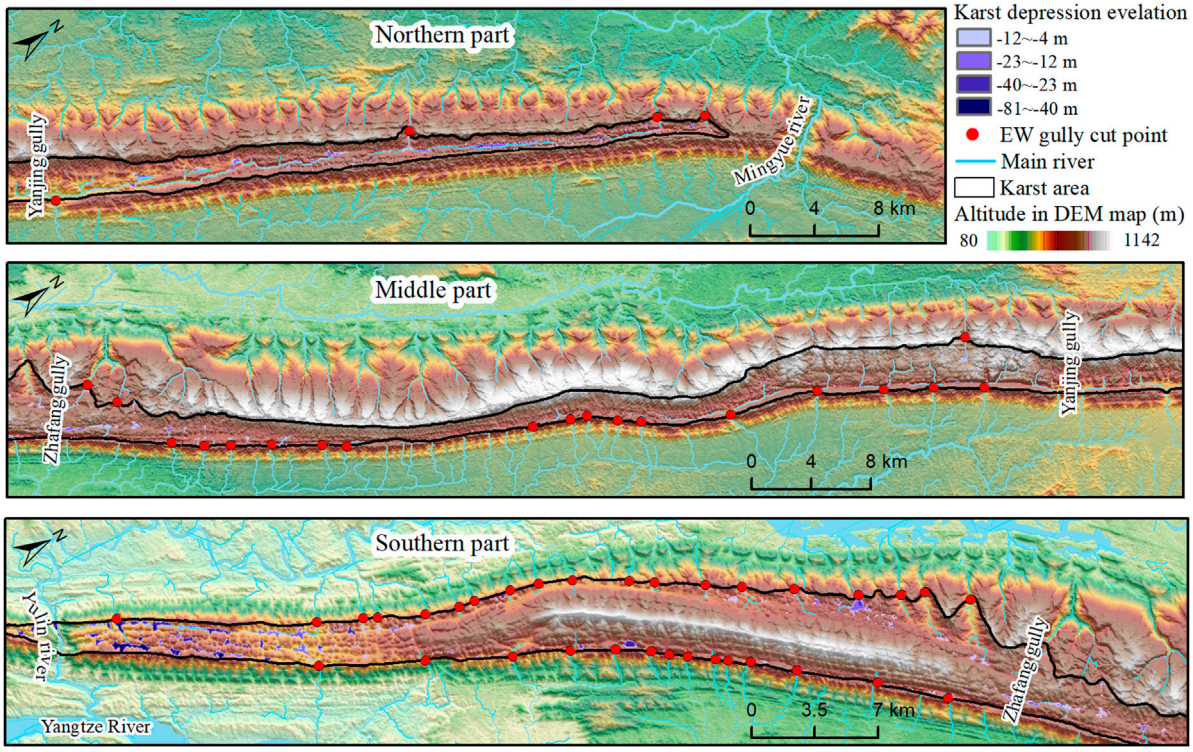

FIGURE 4
Distribution of surface gullies development and karst depressions in Mingyueshan.

TABLE 1 Statistics of EW gullies elevation and density in Mingyueshan.

Area	Lowest elevation (m)		Number of EW gully		Density (number of EW gully/km)	
	East limb	West limb	East limb	West limb	East limb	West limb
Mingyue river to Yanjing gully	488	662.6	1	3	0.021	0.063
Yanjing gully to Zhafang gully	517.9	472	16	3	0.230	0.041
Zhafang gully to Yulin river	185	185	14	20	0.263	0.376

Sichuan, the east-west direction transverse gullies that cut into anticline soluble rock play an essential role in discharging nearby karst water, the cutting length and depth determine the ability and control range of discharging groundwater. According to the degree to which the transverse river cuts through the soluble rock strata, it is divided into three types: fully-cut, partly-cut, and uncut gully. Their ability of discharging groundwater also ranks from strong to weak. The fully-cut and partly-cut gullies correspond to the deep and shallow circulation of groundwater respectively. A multilevel groundwater circulation system is formed under the control of combination of drainage base level with different cutting forms. At the dip end of the northern anticline, the Mingyue river valley, with an elevation of 420 m, was developed in the non-solvable rocks of the Xujiahe Formation and did not cut into the karst rocks of the anticline, therefore the Mingyue river valley should not be considered as an effective drainage area for karst water. Yanjing gully and Zhafang gully are the gullies that partly cut into the soluble rock, with the elevations of 488 m and 472 m respectively. Yulin river fully cut into the soluble rock with 185 m elevation and it is the regional drainage base level in the study area. Yanjin gully, Zhafang gully and Yulin river formed the local drainage base level of the water in the Mingyueshan and controlled the local karst landform features and groundwater circulation conditions. According to the spatial location of these drainage base levels, the anticline was divided into north, middle and south sections. The groundwater circulation characteristics of each section will be analyzed later.

4.2 δ^2H and $\delta^{18}O$ isotope analysis

The stable isotope values of the southern group samples are −46.40‰ to −40.70‰ for δ^2H, and −7.59‰ to −6.48‰ for $\delta^{18}O$. The isotope values

10.3389/feart.2023.1120618

TABLE 2 δ^2H and $\delta^{18}O$ isotope information of water samples.

Group	Sample ID	Elevation (m)	δ^2H (‰)	$\delta^{18}O$ (‰)	*d*-excess
Northern	S01 (hot water hole)	523	−58.1	−8.91	13.18
	S02	668	−56.3	−8.46	11.38
	S03	779	−52.5	−8.13	12.54
	S04	743	−49.9	−7.94	13.62
	S05	682	−49.7	−7.81	12.78
	S06	650	−49.2	−7.73	12.64
Middle	S07	615	−49.7	−7.81	12.78
	S08	614	−50.4	−7.92	12.96
	S09	701	−50.2	−7.78	12.04
	S10	656	−47.7	−7.69	13.82
	S11	597	−49.8	−7.85	13.00
Southern	S12	779	−46.4	−7.59	14.32
	S13	743	−43.8	−7.39	15.32
	S14	672	−45	−7.36	13.88
	S15	647	−46.2	−7.52	13.96
	S16	507	−41.5	−6.69	12.02
	S17	530	−42.2	−6.58	10.44
	S18	638	−46.2	−7.44	13.32
	S19	513	−44.2	−7.08	12.44
	S20	658	−45.2	−7.51	14.88
	S21	647	−44.6	−7.43	14.84
	S22	600	−43.8	−7.19	13.72
	S23	626	−42.6	−6.93	12.84
	S24	542	−40.7	−6.48	11.14
	S25	507	−41.7	−6.69	11.82
	S26	507	−41.4	−6.53	10.84
	S27	507	−41.6	−6.52	10.56
	S28	218	−40.9	−6.59	11.82

of the middle group varied between −50.40‰ and −47.70‰-for δ^2H, from −7.92‰ to −7.69‰ for $\delta^{18}O$. The δ^2H values of the northern group ranges from −58.10‰ to −49.20‰, $\delta^{18}O$ ranges from −8.910‰ to −7.730‰ (Table 2). A binary scatter plots of δ^2H and $\delta^{18}O$ were drawn from 28 sets of isotopic data of water samples in the north, middle and south parts of the Mingyueshan (Figure 5). The samples are between the global meteoric water line (GMWL: $\delta^2H = 8.14 \times \delta^{18}O + 10.9$; Craig 1961) and the local meteoric water line (LMWL: $\delta^2H = 7.85 \times \delta^{18}O + 14.12$; Wen 2017), indicating that there is a close relationship between the recharge source of the samples and atmospheric precipitation. It also reflects that the region is inland far from the steam source and at a high altitude, which is consistent with the actual situation in the study area.

In general, the terrain of Mingyue Mountain decreases from north to south, the average elevation of water samples in the northern and middle sections is generally higher than the southern section. The stable isotope is affected by the altitude, the southern section of Mingyueshan shows obvious subdivision compared with the northern and middle sections: the water samples in the south section are concentrated in the upper right of the scatter diagram, are distributed obviously denser in heavy isotopes $\delta^{18}O$ and δ^2H than those in the middle and north sections. The slope of stable isotope linear curves of the middle and northern group is parallel to that of LMWL and GMWL, which reflects wet climate and weak evaporation in the study area. However, the slope of isotope linear curve of the southern group is significantly less than that of LMWL and GMWL, showing positive $\delta^{18}O$ deviation, which results from the water-rock interaction. The content of δ^2H in rocks is very low, which is not enough to significantly affect the δ^2H value in water, while the rocks are more enriched in $\delta^{18}O$ than water (Pu, 2013). The long-term retention of karst water in the aquifer leads to the enhancement of

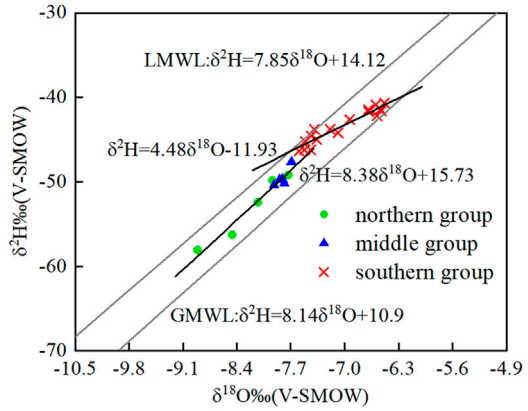

FIGURE 5
Isotopes δ^2H and $\delta^{18}O$ binary graph.

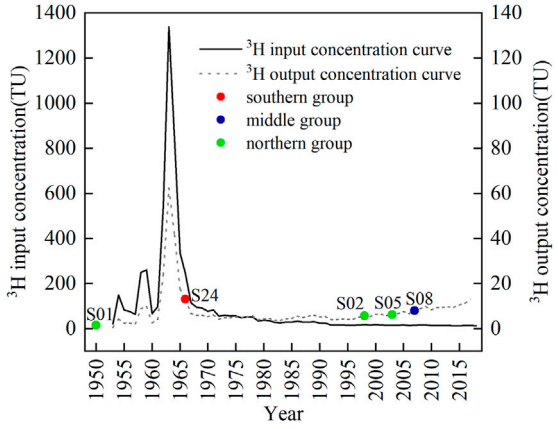

FIGURE 6
^3H input concentration in precipitation and ^3H output concentration curves.

water-rock interaction in the system, $\delta^{18}O$ in the rock will transfer to the water, resulting in $\delta^{18}O$ enrichment in the southern group. It is inferred that the south section groundwater has larger exchange capacity of material components than middle and north sections, and the groundwater circulation in the southern section is deeper than middle and north sections.

4.3 Groundwater residence time

^3H input concentration in precipitation curved graph and ^3H output concentration curved graph from the PEM in study area were established (Figure 6). S01, S02 and S05 are all in the north section of the anticline. The tritium values of S02 and S05 springs are ranging from 5.58 to 6.1Tu. It is estimated that the groundwater runoff time is roughly 15–20 years and the formation time lies from year 1998 to 2003. S01 is a hot water hole involved in deep circulation and has a low ^3H abundance less than 2. It should have been formed before the nuclear explosion in 1953 and has a long groundwater detention time. S08 is an ascending spring in the middle section of the anticline, the measured tritium value is 7.97Tu, which is presumed to have been formed around year 2007 and the groundwater circulation path is short and shallow. S24 is an outcropping spring in the south section of the anticline with 13.01TU tritium value, the groundwater retention age is relatively long, about 50 years. It is speculated that the groundwater of S24 migrates through the deep circulation system and is discharged to the inner spring mouth in the negative terrain. The estimation of the age of tritium retention in groundwater can provide a reliable basis for the classification of groundwater circulation patterns in Mingyueshan.

4.4 Karst water circulation patterns

The north section is from Mingyue river to Yanjin gully, about 46 km long, with few transverse gullies, undeveloped surface water systems and shallow karst depressions. The main karst landforms on the surface are ridge-shallow troughs. The scale of karst development is weak, in which karst troughs of west limb are not obvious, while karst troughs of the east limb are more apparent. In the north section, due to the large area of non-soluble rock strata exposed by the overturning of the anticline, the penetrating valley of Mingyue river does not cut into the soluble rocks, as a result it does not act as an effective drainage area for the inland water of the anticline. Retention time of S02 and S05 spring are short, accompanied with weak water-rock reaction, corresponding to shallow circulation. While the sampling depth of S01 hot water borehole is deep, the groundwater ^3H dating is old and the retention time is long. It is speculated that the overall flow of groundwater in this section is from north to south, the shallow groundwater is discharged through the deep transverse gullies of Yanjing gully, the deep groundwater migrates to the Yulin river. Under the control of the depth and drainage capacity of the deep transverse gullies, there are almost no other transverse gullies development in a certain range near this area. The groundwater in this section is mainly controlled by a single deep transverse gully, which is a unidirectional shallow circulation pattern (Figure 7).

The middle section is from Yanjin gully to Zhafang gully, about 70 km long. The karst landforms developed in this section are ridge-single troughs. The soluble rock strata of Leikoupo and Jialingjiang Formation formed valleys after dissolution, while the non-carbonate rocks on both limbs formed monocline ridge. The structural stress in the middle section is not distributed evenly, resulting in asymmetry between the two limbs of the anticline. To be more concrete, the Xujiahe Formation in the west limb stands up and goes inverted, with steepness occurring in parts of the area. The dip angle of east limb formation is gentle, forming a single plane structure. In this area, the outcrop of Xujiahe Formation is thin, which is vulnerable to the trace-back erosion of cross-cut gullies and cut into the core of the anticline. Rainfall is mainly discharged by lateral runoff from the west limb to the east limb gullies through slope flows, forming deep circulating karst water within a certain depth range below the drainage base level, and leading to longitudinal runoff to the Yulin river. Far away from the control area of fully cut valley, the non-soluble rock strata formation holding karst layer groups are cut open by transverse gullies, as the main drainage channel of groundwater in karst trough valleys. With the continuous tractive erosion of groundwater, the groundwater between adjacent gullies and valleys continuously attacks and

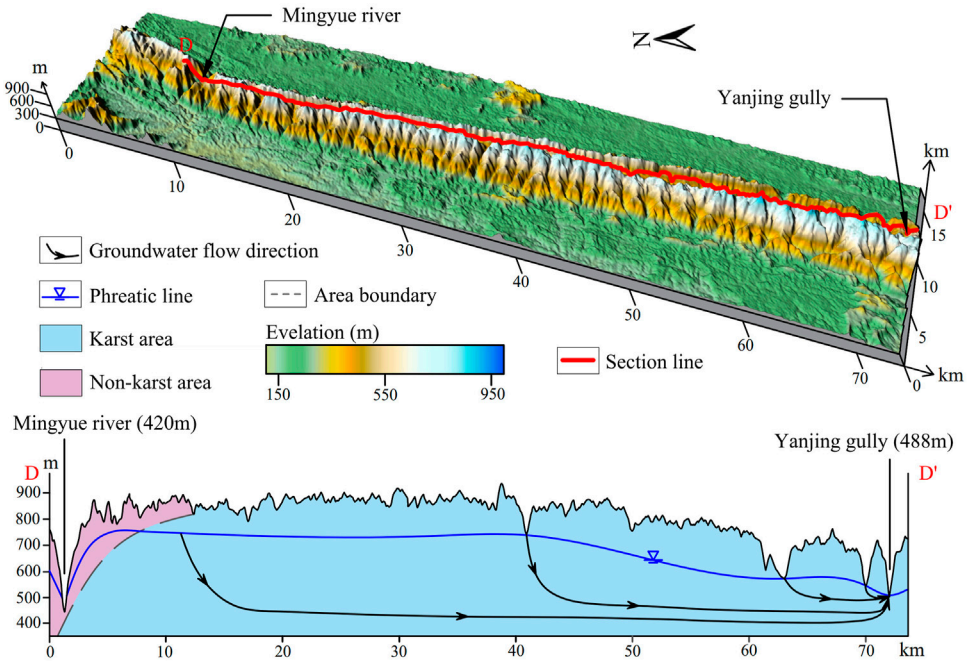

FIGURE 7
Karst water circulation pattern in north section of Mingyueshan.

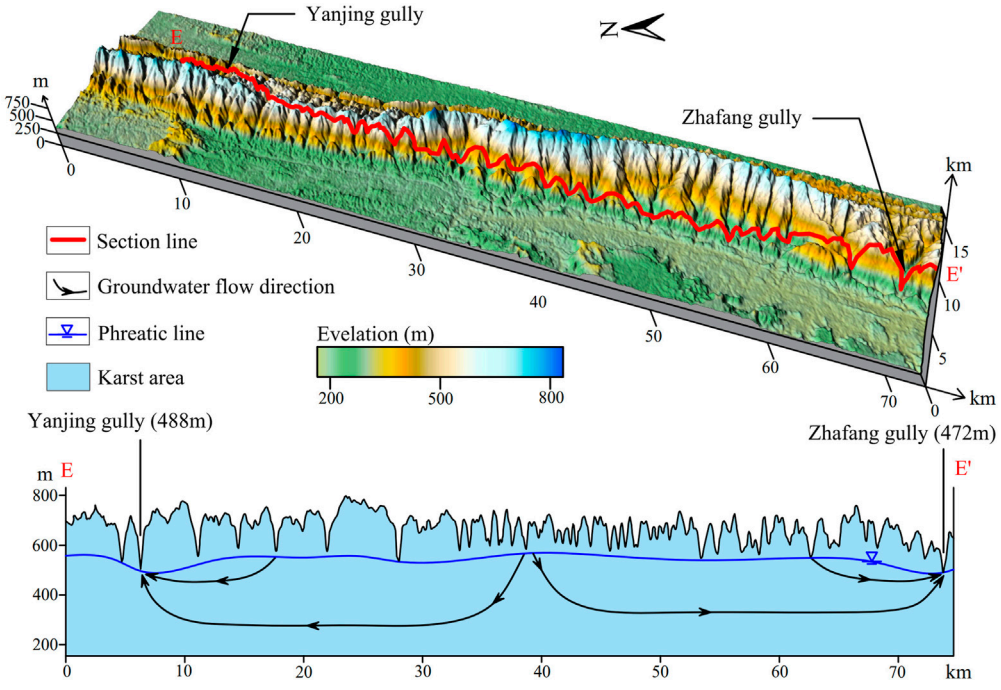

FIGURE 8
Karst water circulation pattern in middle section of Mingyueshan.

merges with each other, leading to the increasing difference in the depth and shallow degree of the transverse gully development. In the development of a series of shallow transverse gullies, a deep cutting gully with a large control range appeared, which controls the discharge of groundwater in the trough valley together with the shallow transverse gullies. Isotope sampling data from the middle section

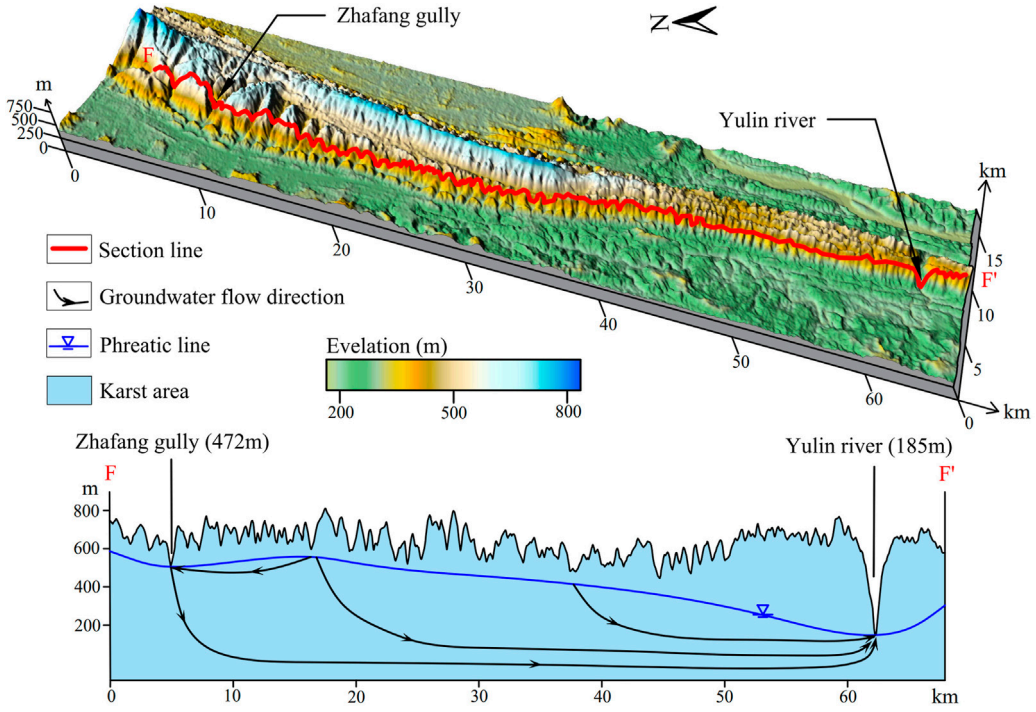

FIGURE 9
Karst water circulation pattern in south section of Mingyueshan.

indicate weak water-rock interaction and a short groundwater retention age. The groundwater in the middle section is jointly controlled by the two partly cut transverse gullies Yanjing gully and Zhafang gully, forming a bidirectional shallow circulation pattern (Figure 8).

The south section is from Zhafang gully to Yulin river, with a length about 54 km. The karst landforms, mainly ridge-double troughs and transverse gullies and valleys, are developed along both limbs of the anticline. The karst depressions are distributed roughly in a beaded shape, the bottom elevation of the depressions decreases from north to south. In this section, the rainfall in the trough valleys is discharged to the syncline area through the cross-cutting gullies on both sides. Meanwhile, due to the development of the surface karst negative terrain in this section, the atmospheric rainfall is rapidly introduced into the underground through the negative terrain, and is discharged along the east-west trough valleys of the anticline to the southern side of the Yulin river. Impacted by the tectonic stress extrusion in the south section, the Feixianguan Formation and Changxing Formation exposed in the core, controlled by the non-soluble rocks of the Feixianguan Formation, the hydraulic connection between the east and west limbs of the anticline is hindered, with a manifestation that the shallow groundwater is mainly discharged through partly cut transverse gullies. In a certain range away from the fully cut valley, where groundwater circulation has not adapted to the valley down-cutting, the valley has a weak influence on the transverse valleys, resulting in the strong development of transverse gullies and valleys and forming shallow depth of groundwater level. Groundwater, is discharged through the shallow transverse gullies, with a small amount of groundwater circulating deeply through the deep dissolution gap. For areas close to the Yulin river, under the control of crustal uplift, fully cut river valley continues to cut down, which controls the groundwater circulation to the deep, leading to a deep depth of groundwater level. When groundwater circulation is adapted to the down-cutting of fully cut valleys, there is basically no gully development on the surface, transverse gullies and valleys will lose the discharge ability. The stable isotopes of the water samples data in the southern section far away from the Yulin River basically fall on the LMWL, indicating that the groundwater is excreted by temporary runoff and belongs to shallow circulation. The stable isotopes of the water samples to the south showed a trend of $\delta^{18}O$ enrichment, the ^{3}H dating also showed that the groundwater retention time was long, which was a deep circulation area. It's inferred that the fully-cut Yulin river valley and partly-cut Zhangfang gully together constitute a multilevel discharge base level of karst water, thus forming a unidirectional shallow-deep nested circulation system jointly controlled by fully cut river valley and partly cut gully (Figure 9).

Under the special conditions of the east Sichuan Basin, where a series of NNE–SSW trending Jura-type folds developed, we considered that the near east-west (EW) direction gullies determine the drainage of karst water largely. In this study, according to the degree of transverse gullies cutting through the soluble rock strata, it can be divided into three types: fully-cut, partly-cut, and uncut gully. Based on geomorphic and environmental isotopes analysis, the karst water circulation under the control of multiple drainage base levels and their combinations is discussed in typical Jura-type fold Mingyueshan. However, these discussions are essentially qualitative, some numerical simulations of groundwater flow can be considered in

future work. The combination of numerical simulation and field data helps to determine the groundwater flow system quantitatively.

5 Conclusion

Under the special tectonic conditions of the Jura-type folds in eastern Sichuan, the down-cutting degree and depth of the near EW gully cutting into soluble rocks determine the drainage capacity of groundwater in the anticline area. According to the morphology of transverse gullies which cut into the soluble rocks in anticline area, transverse gullies can be divided into three types: fully-cut, partly-cut, and uncut. The transverse gullies with different combinations control the shallow circulation and deep circulation of karst water. In this study, the geological and natural geographical factors that control the karst water circulation in the Mingyueshan area were analyzed from the geographical three-dimensional perspective. The groundwater flow system was built by GIS, the direct evidence of the karst water circulation was obtained by the environmental isotopes (δ^2H, δ^{18}O, δ^3H) methods. Based on the above, the karst water circulation patterns under the control of different drainage base levels were explored. It is concluded that the north section of Mingyueshan is a unidirectional shallow circulation pattern controlled by a partly-cut gully. The middle section is a bidirectional shallow circulation pattern controlled by two partly-cut gullies. The karst water circulation in the south section is controlled by a fully-cut gully and a partly-cut gully and forms a unidirectional shallow-deep nested circulation system pattern.

Data availability statement

The original contributions presented in the study are included in the article/supplementary material, further inquiries can be directed to the corresponding author.

Author contributions

ZQ: Conceptualization, writing-original draft, methodology, investigation, formal analysis, and visualization; QZ: Conceptualization, resources, supervision, validation, writing-review and editing; SY: Writing-original draft, methodology, and visualization; YY: writing-review and editing; JZ: Validation and data curation; MX: Resources and supervision; YL: Data curation; ML: Investigation; MN: Investigation. All authors contributed to the article and approved the submitted version.

Funding

This study was supported by the National Natural Science Foundation of China's project under No. 42272318.

Conflict of interest

Authors ML and MN are employed by Chongqing Urban Construction Investment (Group) Co., Ltd.

The remaining authors declare that the research was conducted in the absence of any commercial or financial relationships that could be construed as a potential conflict of interest.

Publisher's note

All claims expressed in this article are solely those of the authors and do not necessarily represent those of their affiliated organizations, or those of the publisher, the editors and the reviewers. Any product that may be evaluated in this article, or claim that may be made by its manufacturer, is not guaranteed or endorsed by the publisher.

References

Cauquoin, A., Jean, B. P., Risi, C., Fourre, E., and Landais, A. (2017). Modeling the global bomb tritium transient signal with the AGCM LMDZ-iso: A method to evaluate aspects of the hydrological cycle. *J. Geophys. Res.* 121 (21), 12612–12629. doi:10.1002/2016JD025484

Charvet, J. (2013). The neoproterozoic-early paleozoic tectonic evolution of the South China block: An overview. *J. Asian Earth Sci.* 74, 198–209. doi:10.1016/j.jseaes.2013.02.015

Chen, K. L., Wu, H. N., Cheng, W. C., Zhang, Z., and Chen, J. (2016). Geological characteristics of strata in Chongqing, China, and mitigation of the environmental impacts of tunneling-induced geo-hazards. *Environ. Earth Sci.* 76 (1), 10–16. doi:10.1007/s12665-016-6325-7

Chen, S., Tang, Z. H., Wang, J., Wu, J. L., Yang, C., Kang, W. L., et al. (2020). Multivariate analysis and geochemical signatures of shallow groundwater in the main urban area of chongqing, southwestern China. *Water* 12 (2833), 2833. doi:10.3390/w12102833

Craig, H. (1961). Isotopic variations in meteoric waters. *Science* 133, 1702–1703. doi:10.1126/science.133.3465.1702

Davis, G. H. (1980). Structural characteristics of metamorphic core complexes. *South. Ariz. Geol. Soc. Am. Memoirs,Cordilleran Metamorph. Core Complexes* 153, 35–77. doi:10.1130/MEM153-p35

Deng, X., Xing, M., Yu, M., Zhao, Z. H., Li, C. S., and Su, Q. W. (2022). Characteristics of the water cycle of Jinan karst spring in northern China. *Water Pract. Technol.* 17 (7), 1470–1489. doi:10.2166/wpt.2022.075

Doney, S. C., Glover, D. M., and Jenkins, W. J. (1992). A model function of the global bomb tritium distribution in precipitation, 1960-1986. *J. Geophys. Res.* 97 (C4), 5481–5492. doi:10.1029/92JC00015

Ford, D., and Williams, P. D. (2007). *Karst hydrogeology and geomorphology*. Hoboken, NJ: John Wiely & Sons.

Gil-Marquez, J. M., Andreo, B., and Mudarra, M. (2019). Combining hydrodynamics, hydrochemistry, and environmental isotopes to understand the hydrogeological functioning of evaporite-karst springs. An example from southern Spain. *J. Hydrology* 576, 299–314. doi:10.1016/j.jhydrol.2019.06.055

Gleeson, T., Befus, K. M., Jasechko, S., Luijendijk, E., and Cardenas, B. M. (2016). The global volume and distribution of modern groundwater. *Nat. Geosci.* 9 (2), 161–167. doi:10.1038/ngeo2590

Hill, C. A., and Polyak, V. J. (2010). Karst hydrology of grand canyon, Arizona, USA. *J. Hydrology* 390 (3-4), 169–181. doi:10.1016/j.jhydrol.2010.06.040

Kattan, Z. (1997). Environmental isotope study of the major karst springs in damascus limestone aquifer systems: Case of the figeh and barada springs. *J. Hydrology* 193, 161–182. doi:10.1016/S0022-1694(96)03137-X

Kaufman, A., Bar-Matthews, M., Ayalon, A., and Carmi, I. (2003). The vadose flow above soreq cave, Israel: A tritium study of the cave waters. *J. Hydrology* 273, 155–163. doi:10.1016/S0022-1694(02)00394-3

Koster, R. D., Broecker, W. S., Jouzel, J., Suozzo, R. J., Russell, G. L., Rind, D., et al. (1989). The global geochemistry of bomb-produced tritium: General circulation model compared to available observations and traditional interpretations. *J. Geophys. Res. Atmos.* 94 (D15), 18305–18326. doi:10.1029/JD094iD15p18305

Laubscher, H. P. (1977). Fold development in the Jura. *Tectonophysics* 37 (4), 337–362. doi:10.1016/0040-1951(77)90056-7

Liang, X., Zhang, R. Q., Luo, M. M., Sun, R. Q., Jin, M. G., Zhou, H., et al. (2022). Discussion on methodology in research of groundwater flow system: A review of research on groundwater flow systems at CUG-wuhan. *Bull. Geol. Sci. Technol.* 41 (01), 30–42. (In Chinese and English Abstract). doi:10.19509/j.cnki.dzkq.2022.0005

Liang, X., Zhang, R. Q., Niu, H., Jin, M. G., and Sun, R. L. (2012). Development of the theory and research method of groundwater flow system. *Bull. Geol. Sci. Technol.* 31 (05), 143–151. (In Chinese and English Abstract).

Liu, R. T., Wang, J. G., Zhan, H. B., Chen, Z., Li, W. J., Yang, D., et al. (2021). Influence of thick karst vadose zone on aquifer recharge in karst formations. *J. Hydrol.* 592, 125791. doi:10.1016/j.jhydrol.2020.125791

Lorette, G., Lastennet, R., Nicolas, P., and Denis, A. (2018). Groundwater-flow characterization in a multilayered karst aquifer on the edge of a sedimentary basin in Western France. *J. Hydrology* 566, 137–149. doi:10.1016/j.jhydrol.2018.09.017

Lu, G., Zhao, L., Zheng, T., and Kaus, P. (2014). Strong intracontinental lithospheric deformation in south China: Implications from seismic observations and geodynamic modeling. *J. Asian Earth Sci.* 86, 106–116. doi:10.1016/j.jseaes.2013.08.020

Lucas, L., and Unterweger, M. P. (2000). Comprehensive review and critical evaluation of the half-life of tritium. *J. Res. Natl. Inst. Stand. Technol.* 105, 541–549. doi:10.6028/jres.105.043

Ma, J. F., Li, X. L., Liu, F., Fu, C. C., Zhang, C. C., Bai, Z. X., et al. (2022). Application of hydrochemical and isotopic data to determine the origin and circulation conditions of karst groundwater in an alpine and gorge region in the qinghai–xizang plateau: A case study of genie mountain. *Environ. Earth Sci.* 81 (10), 291–309. doi:10.1007/s12665-022-10414-9

Meng, X., Xiong, L. Y., Yang, X. W., Yang, B. S., and Tang, G. A. (2018). A terrain openness index for the extraction of karst Fenglin and Fengcong landform units from DEMs. *J. Mt. Sci.* 15 (4), 752–764. doi:10.1007/s11629-017-4742-z

Michel, R. L. (1989). Tritium deposition in the continental United States, 1953-1983. *J. Fujian Agric. For. Univ.* 179, 107–115. doi:10.1002/pola.27791

Nir, A. (1964). On the interpretation of tritium 'age' measurements of groundwater. *J. Geophys. Res.* 69 (12), 2589–2595. doi:10.1029/JZ069i012p02589

Pavel, B., Michal, V., Ludovit, G., and Jozef, M. (2016). Josvafo paleo-polje: Morphology and relation to the landform evolution of aggtelek karst and josva river valley, Hungary. *Z. Fur Geomorphol.* 60 (3), 219–235. doi:10.1127/zfg/2016/0212

Pu, J. B., Cao, M., Zhang, Y. Z., Yuan, D. X., and Zhao, H. P. (2014). Hydrochemical indications of human impact on karst groundwater in a subtropical karst area, Chongqing, China. *Environ. Earth Sci.* 72 (5), 1683–1695. doi:10.1007/s12665-014-3073-4

Pu, J. B. (2013). Hydrogen and oxygen isotope geochemistry of karst groundwater in chongqing. *Acta Geosci. Sin.* 34 (6), 713–722. (In Chinese and English Abstract). doi:10.3975/cagsb.2013.06.08

Rich, J. L. (1934). Mechanics of low-angle overthrust faulting as illustrated by Cumberland thrust block, Virginia, Kentucky, and Tennessee. *AAPG Bull.* 18, 1584–1596. doi:10.1306/3D932C94-16B1-11D7-8645000102C1865D

Silva, A., and Cota, S. (2021). Groundwater age dating using single and time-series data of environmental tritium in the Moeda Synclyne, Quadrilátero Ferrífero, Minas Gerais, Brazil. *J. S. Am. Earth Sci.* 107, 103009. doi:10.1016/j.jsames.2020.103009

Solomon, D. K., and Sudicky, E. A. (1991). Tritium and helium 3 isotope ratios for direct estimation of spatial variations in groundwater recharge. *Water Resour. Res.* 27 (9), 2309–2319. doi:10.1029/91WR01446

Stringfield, V. T., Rapp, J. R., and Anders, R. B. (1979). Effects of karst and geologic structure on the circulation of water and permeability in carbonate aquifers. *J. Hydrology* 12, 313–332. doi:10.1016/0022-1694(79)90178-1

Suppe, J. (1983). Geometry and kinematics of fault-bend folding. *Am. J. Sci.* 283, 684–721. doi:10.2475/ajs.283.7.684

Szczygieł, J., Golicz, M., Hercman, H., and Lynch, E. (2018). Geological constraints on cave development in the plateau-gorge karst of South China (Wulong, Chongqing). *Geomorphology* 304, 50–63. doi:10.1016/j.geomorph.2017.12.033

Taylor, C. B. (1966). Tritium in southern hemisphere precipitation 1953-1964. *Tellus* 18, 105–131. doi:10.1111/j.2153-3490.1966.tb01449.x

Torresan, F., Fabbri, P., Piccinini, L., Dalla, L. N., Pola, M., and Zampieri, D. (2020). Defining the hydrogeological behavior of karst springs through an integrated analysis: A case study in the berici mountains area (vicenza, NE Italy). *J. Hydrology* 28, 1229–1247. doi:10.1007/s10040-020-02122-0

Tóth, J. (1963). A theoretical analysis of groundwater flow in small drainage basins. *J. Geophys. Res.* 68 (16), 4795–4812. doi:10.1029/JZ068i016p04795

Tóth, J. (1962). A theory of groundwater motion in small drainage basins in central Alberta, Canada. *J. Geophys. Res.* 67 (11), 4375–4388. doi:10.1029/JZ067i011p04375

Tóth, J. (2009). *Gravitational system of groundwater: Theory evaluation, utilization*. New York: Cambridge University Press.

Tóth, J. (1999). Groundwater as a geologic agent: An overview of the causes, processes, and manifestations. *Hydrogeology J.* 7 (1), 1–14. doi:10.1007/s100400050176

Vasic, L., Palcsu, L., and Fen, H. (2019). Groundwater gravitational circulation of karst veliko vrelo and malo vrelo springs by isotope and the noble gas method: Case study of the beljanica massif. *Environ. Earth Sci.* 78 (10), 307–314. doi:10.1007/s12665-019-8294-0

Wang, Y. S., Xu, M., Yang, Y. N., Xia, Q., Jiang, B., Yang, C., et al. (2022). Structural characteristics and deformation evolution of an intra-continental fold-thrust belt in eastern sichuan: Insights into analogue sandbox models. *Front. Earth Sci.* 10, 1–23. doi:10.3389/feart.2022.897882

Wang, Z. X., Zhang, J., Tao, L., Xie, G., and Ma, Z. J. (2010). Structural analysis of the multi-layer detachment folding in eastern sichuan province. *Atca Geol. Sin. Engl. Ed.* 84 (003), 497–514. doi:10.1111/j.1755-6724.2010.00269.x

Wang, Z. X., Zhang, J., Tao, L., Zhou, X. G., Ma, Z. J., Tang, L. G., et al. (2012). Structural traps in detachment folds: A case study from the comb- and troughtrough-like' deformation zone/s, east Sichuan, China. *Atca Geol. Sin. Engl. Ed.* 86 (4), 828–841. doi:10.1111/j.1755-6724.2012.00709.x

Wen, K., and Li, C. X. (2020). The geometry and kinematics of the intersection area of eastern Sichuan and the Dabashan fold-thrust belt. *Atca Geol. Sin. Engl. Ed.* 94, 426–438. doi:10.19762/j.cnki.dizhixuebao.2020005

Wen, Y. R. (2017). *Variations of stable isotope in daily precipitation and the response to the ENSO phases in Chongqing, Southwest, China*. Chongqing: Southwest University. (In Chinese and English Abstract).

Wu, Q. S., Deng, C. B., and Chen, Z. Q. (2016). Automated delineation of karst sinkholes from LiDAR-derived digital elevation models. *Geomorphology* 266, 1–10. doi:10.1016/j.geomorph.2016.05.006

Xiao, Q., Jiang, Y. J., Shen, L. C., and Yuan, D. X. (2018). Origin of calcium sulfate-type water in the triassic carbonate thermal water system in chongqing, China: A chemical and isotopic reconnaissance. *Appl. Geochem.* 89, 49–58. doi:10.1016/j.apgeochem.2017.11.011

Yang, P. H., Luo, D., Groves, C., and Xie, S. Y. (2019). Geochemistry and Genesis of geothermal well water from a carbonate–evaporite aquifer in Chongqing, SW China. *Environ. Earth Sci.* 78, 33. doi:10.1007/s12665-018-8004-3

Yang, P., and Ye, S. J. (2018). Global model of the annual mean concentration of Tritium in precipitation, 1960-2014. *Acta Sci. Circumstantiae* 38 (5), 1759–1767. (In Chinese and English Abstract). doi:10.13671/j.hjkxxb.2017.0475

Zhang, J. R., Yang, P. H., Groves, C., Luo, X. H., and Wang, Y. Y. (2022). Influence of geological structure on the physicochemical properties and occurrence of middle-deep groundwater in Chongqing, Southwest China. *J. Hydrology* 610, 127782. doi:10.1016/j.jhydrol.2022.127782

Zhang, Y. H., Ye, S. J., and Wu, J. C. (2011). A modified global model for predicting the tritium distribution in precipitation, 1960-2005. *Hydrol. Process.* 25 (15), 2379–2392. doi:10.1002/hyp.8001